Process Optimization of Alumina Extraction from Aluminium Dross Via Response Surface Methodology

Mohamad Jamil Arif Mansor[1], Yeoh Yuan Xin[1], Siti Nor Amira Rosli[1], Noor Intan Shafinas Muhammad[2], Shanmuga Kittappa[3] and Sumaiya Zainal Abidin[4,5]*

[1]Faculty of Chemical and Process Engineering Technology, Universiti Malaysia Pahang Al-Sultan Abdullah, Kuantan, Pahang, Malaysia
[2]Faculty of Civil Engineering Technology, Universiti Malaysia Pahang Al-Sultan Abdullah, Kuantan, Pahang, Malaysia
[3]Environmental Preservation and Innovation Centre, Kuala Lumpur, Malaysia
[4]Centre for Research in Advanced Fluid & Processes (FLUID CENTRE), Universiti Malaysia Pahang Al-Sultan Abdullah, Kuantan, Pahang, Malaysia
[5]Faculty of Chemical Engineering, Industrial University of Ho Chi Minh City, Ho Chi Minh City, Vietnam
*Corresponding author (e-mail: sumaiya@umpsa.edu.my)

Despite its toxic nature, aluminium dross (AD), which is composed primarily of aluminium oxide, alloying elements, and salts such as sodium chloride (NaCl) or potassium chloride (KCl), may be repurposed into valuable applications. Various techniques including precipitation, leaching, sol-gel, and hydrothermal methods have been explored for alumina (Al_2O_3) extraction. However, there have been no specific studies reported on process optimization to date. Acid-leaching precipitation, a hydrometallurgical approach, was applied to treat and recover alumina from AD samples in the present study. Response surface methodology (RSM) with Design Expert® (DE) software was employed to optimize alumina production by investigating the interactions of parameters and varying the experimental conditions: temperature, acid concentration, and pH precipitation. X-ray fluorescence (XRF) analysis was used to determine the percentage of alumina recovery from the AD sample. RSM revealed that the acid concentration had a strong effect on alumina yield, while pH significantly influenced its purity. The optimal parameters for alumina extraction were 2.2 M acid concentration, leaching at 71.5 °C, and precipitation at pH 6.5, which gave a maximum yield of 42.17 % and a purity of 91.90 %.

Keywords: Alumina; aluminium dross; optimization; response surface methodology; waste valorization

Aluminium (Al) and its alloys showcase favourable characteristics, including their lightweight nature, excellent electrical conductivity, and resistance to corrosion. These properties have contributed to their extensive usage across various fields, including aerospace, architectural construction, marine, and domestic industries. The growth of the aluminium market, which increased from USD 159.39 billion in 2021 to USD 168.84 billion in 2022, further underscores this trend. Another indicator of the high demand is the growing interest in using recycled aluminium, also known as secondary aluminium (SA). This growing trend is due to its low cost and the significant reduction in energy consumption. SA production boasts a 95 % lower energy intensity than primary production, making it an attractive option for many industries [1]. Recycling scrap metal also holds advantages as it conserves aluminium resources and reduces costs associated with waste landfilling. However, the rise in SA production corresponds to an increase in aluminium dross generation [2].

The production of aluminium dross (AD), a by-product of the smelting process, can be categorized into two main types, namely primary AD (PAD) and secondary AD (SAD). PAD consists of 80 wt.% aluminium content, while SAD consists of 5 – 10 wt.% with the remainder being metal oxide and salts [3]. The remaining substances are primarily composed of oxidized compounds such as alumina (Al_2O_3), ferric oxide (Fe_2O_3), aluminium nitride (AlN), aluminium (Al), cryolite (Na_3AlF_6), silicon (Si), silicon dioxide (SiO_2), aluminium carbide (Al_4C_3), spinel (MgO· alumina), fluoride, and chloride compounds [4,5]. The formation of AD is primarily caused by the presence of impurities in the molten Al. As a result, these impurities react with the salt, leading to the formation of a layer of AD on the top of the molten Al through an oxidation process that was triggered when the molten metal contacted ambient air [6].

The production of AD has become a challenge to the aluminium industry, because for every 1,000 kg

122   Mohamad Jamil Arif Mansor, Yeoh Yuan Xin,
       Siti Nor Amira Rosli, Noor Intan Shafinas Muhammad,
       Shanmuga Kittappa and Sumaiya Zainal Abidin

Process Optimization of Alumina Extraction
from Aluminium Dross Via Response
Surface Methodology

of molten aluminium produced, 15 – 25 % of by-products are produced [7]. Most of the AD is discarded in landfills, posing potential risks such as the release of flammable and poisonous gases such as hydrogen sulphide, hydrogen, phosphine, methane, and ammonia, if the dross reacts with moisture or water [8]. Furthermore, if it seeps into underground water, toxic metal ions may be produced. The toxic properties of dross are the root cause of this issue, which can adversely affect the environment, including groundwater, the ozone layer, and agricultural activities. The accumulation of AD in the environment is poised to increase due to the demand for aluminium. This trend poses a significant challenge for waste management in the industry, and has resulted in a growing global focus on the disposal and recycling of waste aluminium dross.

According to Tsakiridis (2012) [9], and Mahinroosta & Allahverdi (2018) [10], the conversion of AD into a usable product such as Al_2O_3 has various advantages, including the retrieval of valuable metals, the creation of useful end-products, and the mitigation of hazardous materials. Additionally, the process can be economically advantageous as it can minimize disposal costs of AD and provide positive income by the sale of the recovered metals and products. One of the techniques to utilize AD is alumina extraction. In this procedure, the aluminium oxide is separated from the other constituents, including other metal oxides present in the dross. This process is often carried out using various techniques, including chemical treatments, physical separation methods, and thermal processing [11]. Chemical treatment is known to be an effective way to recover alumina from dross, although the efficiency of the process varies according to the type of dross and method used [12]. Implementing this technique may require a significant capital investment, resulting in a relatively high cost.

Several methods of recycling alumina from AD, such as chemical treatments including acid leaching, alkaline leaching, smelting, and electrochemical extraction, have been extensively studied. In the context of aluminium extraction from secondary aluminium dross, research primarily focuses on pyrometallurgical and hydrometallurgical processing methods. However, the pyrometallurgical approach is not preferred due to its high energy consumption as well as the need for relatively high-temperature treatments and reducing agents [13]. On the contrary, the hydrometallurgical approach is universally employed due to its simplicity, cost-effectiveness, and positive environmental impact, making it a promising pathway for future extraction processes and a practical choice for recovering and processing secondary dross [14].

Hydrometallurgical processes for alumina extraction can be achieved using both acidic and alkaline routes, with variations in the leaching process parameters (such as reaction time and temperature) yielding a wide range of results. Although both acid and alkaline leaching can be utilized, acid leaching has demonstrated superior effectiveness in aluminium extraction compared to alkaline leaching. This approach is widely adopted due to its simplicity, cost-effectiveness and favourable environmental impact, making it a promising option for future extraction processes and a feasible solution for recovering and processing SAD [15]. A study by Dash et al. (2008) investigated the impact of acid dissolution on alumina extracted from white aluminium dross. Their findings demonstrated a notable dissolution of alumina, reaching approximately 95 %, at concentrations ranging between 20 – 40 % (v/v). Mahinroosta & Allahverdi (2018) achieved a purity of 98 % using hydrochloric acid under optimal conditions which were 85 °C, an acid concentration of 5 M and 120 minutes reaction time [16]. In a recent investigation, Shi et al. (2023) managed to attain 99.5 % alumina purity by employing sulfuric acid as the leaching agent [17]. This was accomplished at 90 °C leaching temperature, a leaching duration of 3 hours with 30 wt.% H_2SO_4 solution, and a liquid to solid ratio (L/S) of 10. These findings strongly suggest that utilizing acid as a leaching agent in the hydrometallurgical process offers advantages, as it has been proven to lead to higher purity alumina.

Although there are numerous potential advantages in extracting alumina from aluminium dross, there are still some challenges that need to be addressed. According to the study by Mahinroosta & Allahverdi (2018), the presence of other metals in the dross can impede the process of alumina extraction, resulting in the reduced purity of the yield [16]. This underscores the importance of developing effective strategies to minimize the impact of these impurities while improving the extraction process to ensure the production of high-quality pure alumina [16]. Furthermore, it is important to emphasize the scarcity of existing research on optimizing the process of alumina extraction from aluminium dross. This is because optimization can be used to shorten the time and avoid ineffective parameters and errors in the process. One of the optimization techniques that is commonly used in research is response surface methodology (RSM), which utilizes both mathematical modelling and experimental design to obtain a precise prediction of experimental performance.

At present, extensive research is done by focusing on the extraction process utilizing RSM. The objective is to enhance the leaching processes of valuable metals such as silver, zinc, and copper [18–20]. For instance, the study by Kolbadinejad and Ghaemi (2024) applied RSM to optimize the acid leaching extraction process [21]. Their research revealed that the predictive conditions obtained from RSM achieved high recovery rates of cadmium and zinc from low-grade waste. These conditions extracted 86.13 - 89.61 % of zinc. Similar results can be seen in the study conducted by Wei et al. (2023) in which the optimum conditions for extracting valuable metals from the waste of light-emitting diodes (LED) were

123 Mohamad Jamil Arif Mansor, Yeoh Yuan Xin,
Siti Nor Amira Rosli, Noor Intan Shafinas Muhammad,
Shanmuga Kittappa and Sumaiya Zainal Abidin

Process Optimization of Alumina Extraction
from Aluminium Dross Via Response
Surface Methodology

found to be a temperature of 80.4 ℃, acid concentration of 3.1 mol/L and a leaching period of 5 h [19]. The data revealed that approximately 99.55 % of copper (Cu) and 99.36 % of silver (Ag) were extracted, respectively. These findings indicate that RSM is capable of making predictions that produce a good impact on the extraction process. Nonetheless, the optimization of alumina extraction from AD has yet to be reported in other studies. Therefore, the main objective of this paper was to study the relationship between each parameter by optimizing the leaching temperature, pH value for precipitation, and acid concentration, in order to maximize extraction yield and alumina purity. This was conducted using RSM based on the central composite design (CCD) in DE software. This statistical approach predicts favourable conditions and optimizes processes, thus contributing to research efforts to drive advancements in AD recycling.

EXPERIMENTAL

1. Materials

The AD used in this experiment, specifically SAD, was acquired from a waste collection centre located in Malaysia. The sulfuric acid used was supplied by Sigma Aldrich in Malaysia and had a purity of 98 %. Ammonia solutions with a purity of 28 – 30 % were supplied by Merck and the deionized water used in this experiment was treated by PURELAB Quest ELGA.

2. Response Surface Methodology (Design Expert RSM)

A central composite design (CCD) and DE software were utilized to optimize the alumina extraction process. The CCD consisted of 17 experimental runs with three-star points. The experimental design included the centre point, factorial points (± 1), axial points (± α), and three replicates at the centre points. The experimental runs were randomized to avoid any potential bias. The yield and purity of the extracted alumina were recorded for each experimental run. Table 1 summarizes the DE software inputs, which include parameter ranges determined based on previous experiments and a literature review. Multiple factors such as leaching temperature, concentration of sulfuric acid and pH for precipitation were considered to establish the most favourable extraction conditions.

The methodological approach for this study was primarily based on the framework established by How et al. (2017), which involved using an acid concentration of 2 M and a leaching temperature of 70 °C, while varying the pH level between 5 and 9 [22]. This approach was subsequently adapted and modified in studies conducted by Roslan et al. (2019) [23] and Mohamad et al. (2022) [24].

3. Extraction of Alumina by a Hydrometallurgical Technique

Alumina (Al_2O_3) was extracted from aluminium dross (AD) using the acid-leaching precipitation method, which involved four main steps: chloride washing, acid leaching, ammonia precipitation, and calcination. Initially, the washing method was used to eliminate chloride salts and other soluble chemicals present in the AD. For thorough elimination of chlorides, 25 grams of AD were mixed with 100 mL DI water. The mixture was stirred at 500 rpm using an overhead stirrer for 40 minutes before being allowed to settle for 20 minutes, and this process was repeated six times. The liquid residue was filtered, and Mohr's method was applied to evaluate the chloride content. This was done to ensure complete elimination of chloride in the AD [7,25]. The sample was then dehydrated for 12 hours at 110 °C. Next, acid leaching was employed to recover the Al_2O_3 in the form of aluminium sulphate from the AD. The procedure was started by mixing 25 grams of the washed AD in a beaker with 100 mL of sulfuric acid (H_2SO_4) at different concentrations (1 M, 1.5 M, 2 M, 2.5 M, and 3 M). The leaching process was carried out at various temperatures (60 °C, 65 °C, 70 °C, 75 °C, and 80 °C) for an hour, while being stirred at a speed of 400 rpm. The mixture was then cooled to room temperature and left to settle for 18 hours. As the solid particles settled, the solution became clear. Ammonia was then added to the clear solution until a pH of 7 was attained, causing precipitation. The solution was stirred for 30 minutes until the hydroxide precipitate formed a milky white solution. The mixture then underwent a 20-minute centrifugation process. In preparation for the calcination step, the collected white precipitate was subjected to a washing procedure using deionized water. The purpose of this step was to remove any unreacted leaching solution containing ammonia that might have adhered to the precipitate. After that, the precipitate was dehydrated for 18 hours at 110 °C. Finally, the samples were calcined at 700 °C for 6 hours in a furnace, resulting in the formation of a white powder, which was alumina (Al_2O_3).

Table 1. Parameters and levels of the central composite design experiment.

No	Parameter	Unit	Code	Type of Factor	Actual value of coded levels				
					-α	-1	0	+1	+α
1	Temperature	°C	A	Numerical	60	65	70	75	80
2	Concentration	M	B	Numerical	1	1.5	2	2.5	3
3	pH precipitation	pH	C	Numerical	5	6	7	8	9

124   Mohamad Jamil Arif Mansor, Yeoh Yuan Xin,
     Siti Nor Amira Rosli, Noor Intan Shafinas Muhammad,
     Shanmuga Kittappa and Sumaiya Zainal Abidin

Process Optimization of Alumina Extraction
from Aluminium Dross Via Response
Surface Methodology

Equations (1) – (5) below demonstrate the potential reactions that occur during the leaching process following the reaction of AD with sulfuric acid. In addition, the precipitation process involving ammonia takes place following the collection of leachates from the leaching process.

$$Al_2O_3 + 3H_2SO_4 \rightarrow Al_2(SO_4)_3 + 3H_2O \quad (1)$$

$$Al_4C_3 + 6H_2SO_4 \rightarrow 3CH_4 + 2Al_2(SO_4)_3 \quad (2)$$

$$2AlN + 4H_2SO_4 \rightarrow Al_2(SO_4)_3(NH_4)_2SO_4 \quad (3)$$

$$AlN + 4H_2O \rightarrow Al(OH)_3 + NH_4OH \quad (4)$$

$$10NH_4OH + 3Al_2(SO_4)_3 + 5H_2O \rightarrow$$
$$Al_6(OH)_{10}(SO_4)_4.5H_2O + 5(NH_4)_2SO_4 \quad (5)$$
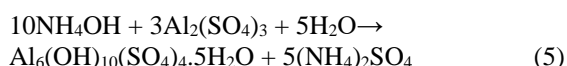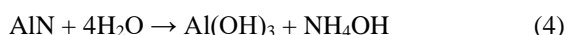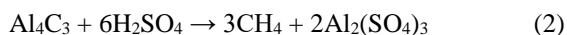
Equation (6) further elucidates the central reaction involved in the precipitation process, where ammonia reacts to produce aluminium hydroxide.

$$Al_2(SO_4)_3 + 6\ NH_3 \cdot H_2O \rightarrow 2Al(OH)_3 + 3(NH_4)_2SO_4 \quad (6)$$

Lastly, Equation (7) illustrates the decomposition of aluminium hydroxide to alumina during the calcination process.

$$2Al(OH)_3 + Heat \rightarrow Al_2O_3 + 3H_2O \quad (7)$$
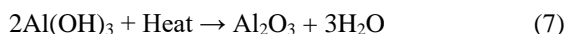
4.   Yield Calculation

Calculation of the yield was based on Equation (8) as follows:

$$Extracted\ Yield\ (\%) = \frac{Weight\ of\ End\ Product}{Initial\ Mass\ Aluminium\ Dross} \times 100\% \quad (8)$$

The yield was calculated to assess both the effectiveness of the reaction converting AD into the final product, and the efficiency of the parameter interactions.

5.   Characterization Analysis

X-ray fluorescence (XRF) was used to examine the chemical composition of the samples. The efficiency of the parameters in producing a significant quantity of the end product was evaluated through calculation of the product yield. Other analyses used to determine the physicochemical properties of the extracted alumina were X-ray diffraction (XRD) and the Brunauer-Emmett-Teller (BET) method. A Thermo Scientific QUANT'X XRF was used to analyze the concentrations of elements and corresponding oxides in the sample. The spectrometer setup included an air-cooled X-ray tube with a rhodium anode, capable of delivering up to 50 W power within the voltage range of 4 – 50 kV and current range of 0.02 – 1.98 mA. It also contained a Peltier-cooled silicon (Li) drifted crystal detector with a crystal area of 15 mm², depth of 3.5 mm, and a remarkable 155 eV resolution. Pulse processing was carried out using a 32-bit digital processor offering 20 eV channels, adjustable shaping time (1 – 40 ms), and accommodating live count rates up to 100,000 cps, covering an energy range of 400 – 40,960 eV. Complementary primary X-ray beam filters were positioned strategically for optimized excitation conditions and reduced background interference. Notably, duplicate analyses under vacuum were performed for each sample to ensure precision. Using the Rigaku Miniflex II instrument, the structure and phases of alumina were analyzed by XRD. The Cu monochromatic anode was used in the analysis as a source of X-ray radiation at 30 kV and 15 mA with a wavelength of 1.5418. XRD patterns in the 2θ range of 10°–80° were examined with a slow scan speed of 1° per minute and a step size of 0.02°. BET theory was used to determine the alumina's pore volume and surface area after calcination. Determination of the sample's specific surface area (measured in m^2/g) using gas adsorption analysis involved a multi-point approach, which entailed the continuous passage of an inert gas like nitrogen over the solid sample, or the suspension of the solid sample within a precisely defined volume of gas.

RESULTS AND DISCUSSION

1.   Composition of Aluminium Dross

There were several elements present in the sample of AD, and those identified by XRF analysis were aluminium (Al), iron (Fe), magnesium (Mg), potassium (K), silicon (Si), calcium (Ca), sulfur (S), titanium (Ti), and others. The chemical composition of AD in wt.% is shown in Table 2. These findings indicate that the AD was primarily composed of Al_2O_3.

Table 2. Chemical composition of aluminium dross in wt%.

Oxides								
Al_2O_3	CaO	FeO	MgO	K_2O	SiO	SO_2	TiO_2	Others
88.94	0.69	1.85	1.17	0.55	4.94	0.02	0.45	1.39

125   Mohamad Jamil Arif Mansor, Yeoh Yuan Xin,
     Siti Nor Amira Rosli, Noor Intan Shafinas Muhammad,
     Shanmuga Kittappa and Sumaiya Zainal Abidin

Process Optimization of Alumina Extraction
from Aluminium Dross Via Response
Surface Methodology

Table 3. Experimental parameters and results.

Run	Parameter A: Temperature [°C]	Parameter B: Concentration [M]	Parameter C: pH Precipitation	Response 1: Yield [%]	Response 2: Purity [%]
1	70	2.0	9	32.48	83.12
2	65	1.5	8	22.00	85.12
3	70	2.0	7	44.68	91.34
4	75	1.5	6	28.61	92.95
5	70	2.0	5	30.44	88.20
6	75	2.5	6	36.47	90.88
7	70	2.0	7	42.56	91.79
8	65	2.5	8	31.43	87.04
9	65	1.5	6	27.11	88.69
10	75	2.5	8	37.56	88.32
11	70	2.0	7	45.62	91.69
12	80	2.0	7	29.90	91.78
13	75	1.5	8	25.54	89.09
14	70	3.0	7	38.74	89.93
15	65	2.5	6	35.58	90.30
16	70	1.0	7	16.63	89.29
17	60	2.0	7	24.05	89.83

2.   Response Surface Methodology (RSM) Analysis

The CCD interface of RSM was employed in the experimental design. The data obtained from the experiment was analysed to fit a quadratic model equation derived using the CCD tool. The resulting equation allowed the generation of 3-D response surface plots to visualize the relationships between the input parameters and the response variables [26].

Table 3 presents the experimental design and results for the two responses in each run. It consists of three parameters and two responses that represented the percentage yield and purity of the extracted alumina from multiple experiments. The yield values obtained in these experiments ranged from 16.64 % to 45.62 %, while the purity values were 83.12 % to 92.95 %, with variations based on the specific experimental conditions employed.

2.1.   Effect of Parameters on the Percentage Yield

To comprehensively examine the model's fitness, significance and precision, an intricate statistical analysis of variance (ANOVA) was executed through dedicated software. The ANOVA table shown in Table 4 demonstrated the significance of the model utilized for yield probability (p-value of 0.05), while a poor model fit (p-value > 0.05 or 5 %) provided further evidence of its significance. In the present study, the p-value for the model was 0.0004, which is less than

0.05, indicating that the model was valid. Table 4 identified several significant factors affecting alumina extraction from AD. In this context, five model terms were found to be significant: temperature (A), concentration of acid (B), quadratic term of temperature (A^2), quadratic term of acid concentration (B^2), and quadratic term of pH (C^2). Acid concentration exhibited the highest F-value of 71.54 in the ANOVA table, implying its significant effect on the yield. In addition, pH (C), temperature – acid concentration (AB), temperature – pH (AC), acid concentration – pH (BC), were found to be insignificant in this model.

The lack of fit F-value of 2.96 indicates that the lack of fit was not statistically significant when compared to pure error. This implies that the model adequately fit the data and effectively captured the relationships among the variables under study. There was a 27.17 % chance of a significant lack of fit F-value due to noise. Having a lack of fit value that is not significant is a desirable outcome, as it suggests that the model appropriately explains the data. It indicates that the model fits the data well, which can lead to more accurate conclusions and predictions. The coded equation presented in Equation (9) allows for prediction of the response at a specific factor level based on the significant p-value. In this equation, +1 was designated for high parameter levels, whereas -1 was assigned to low levels. This coded equation facilitated the assessment of the significance of each factor by comparing their coefficients.

126 Mohamad Jamil Arif Mansor, Yeoh Yuan Xin,
      Siti Nor Amira Rosli, Noor Intan Shafinas Muhammad,
      Shanmuga Kittappa and Sumaiya Zainal Abidin

Process Optimization of Alumina Extraction
from Aluminium Dross Via Response
Surface Methodology

Table 4. ANOVA table for yields obtained from (CCD) RSM.

Source	Sum of Squares	df	Mean Square	F-value	p-value	Coefficient Estimate
Model	1007.81	9	111.98	19.07	0.0004	43.5700
A-Temperature	35.34	1	35.34	6.02	0.0439	1.4900
B-Concentration	420.12	1	420.12	71.54	< 0.0001	5.1200
C-pH	3.17	1	3.17	0.54	0.4862	-0.4454
AB	0.51	1	0.51	0.09	0.7775	0.2517
AC	6.69	1	6.69	1.14	0.3211	0.9147
BC	3.30	1	3.30	0.56	0.4777	0.6426
A²	378.01	1	378.01	64.37	< 0.0001	-4.4200
B²	347.93	1	347.93	59.24	0.0001	-4.2400
C²	210.54	1	210.54	35.85	0.0005	-3.3000
Residual	41.11	7	5.87			
Lack of Fit	36.21	5	7.24	2.96	0.2717	
Pure Error	4.90	2	2.45			

In this study, the null hypothesis, which was that the parameters influenced yield values, was accepted or rejected by evaluating p-values. This is because the p value represents the probability of acquiring outcomes as unusual as the observed outcome of a statistical hypothesis test. A p value less than 0.05 suggests that the parameter or model had a significant effect on the process. Thus, a type I hypothesis was applied in this study, implying that the results only had a 5 % or less chance of occurring, if the null hypothesis was true. The quadratic model equation for alumina production as a function of alumina yield (%) with variables A for temperature, B for acid concentration, A^2 for quadratic term of temperature, B^2 for the quadratic term of acid concentration, and C^2 as the quadratic term of pH, is shown in Equation (9).

$$Yield = 43.57 + 1.49A + 5.12B - 4.42A^2 - 4.24B^2 - 3.30\,C^2 \qquad (9)$$

2.2. Response Surface Method Graph for Yield

Figure 1 shows the 3D plots of the response surface methodology (RSM) for three independent parameters influencing the yield of extracted aluminium. Each response surface plot includes two parameters, while the third parameter was held constant at its mean level.

pH Precipitation

Based on the ANOVA's p-value in Table 4 and Figure 2c(iii), pH showed a lack of influence on the yield of alumina extracted. In Figure 2c(iii), the curve is close to being horizontal, which indicates that pH exerted a minimal influence on the yield, which remained notably constant. The yield displayed marginal fluctuations, ranging from 39 to 44, as the pH was adjusted from 6 to 8. This observation is aligned with the pH trends exhibited in Figures 1b(i&ii) and 1c(i&ii). The predominant factor affecting the yield was the concentration of ions present in the leachate. The function of pH precipitation was in converting all ions into solid form, without directly impacting the overall yield.

Acid Concentration

Figure 2b(iii) demonstrates that employing higher acid concentrations led to enhanced yields. This improvement is likely attributed to the solution's corrosive nature, which could be intensified by the higher acidity stemming from increased acid concentrations. Consequently, this increased corrosive property speeds up the leaching process and encourages a higher yield. A comparable outcome is evident in a study by Matinde et al. (2018) where they discovered that increasing the acid concentration initially boosts the effectiveness of alumina extraction [27]. These findings align with the the results in Figure 2b(iii) and other studies, where an increase in the Al leaching rate was observed, rising from 46.2 % to 76.3 % when the acid concentration was increased from 10 wt.% to 20 wt.% [17]. However, the trend showed that once the concentration surpassed 2.3 M, as depicted in Figures 1a(i&ii), 1c(i&ii), and 2b(iii), the yield began to decrease. This trend was consistent with studies by Dash et al. (2008) [3] and Shi et al. (2023) [17], where the leaching rate was reported to decrease when the acid concentration exceeded 30 wt.%. The study by Sarker et al. (2015) also gave a similar result, wherein alumina extraction exhibited an upward trend solely up to an acid concentration of 4 mol/L [28]. Following the attainment of a peak value of 51 %, the rate of extraction declined for acid concentrations surpassing 6 mol/L. This trend can be explained by the relationship between the metal cation concentration in the solution and the acid concentration. There are a few theories as to why this phenomenon happens. Roslan et al. (2019) stated that

127   Mohamad Jamil Arif Mansor, Yeoh Yuan Xin,
       Siti Nor Amira Rosli, Noor Intan Shafinas Muhammad,
       Shanmuga Kittappa and Sumaiya Zainal Abidin

Process Optimization of Alumina Extraction
from Aluminium Dross Via Response
Surface Methodology

the competition between cations and Al^{3+} ions to attract SO^{-} ions may be one of the potential factors that caused the decrease in the abundance of aluminium ions in the solution [23]. Meanwhile, Sarker et al. (2015) [28] and Al-Zahrani and Abdul-Majid (2009) [29] suggested that the presence of Al^{3+} ions could potentially hinder the diffusion of H^{+} ions at higher concentrations. As the concentration increases, the diffusion rate of Al^{3+} ions from the solid material into the solution also escalates, intensifying the diffusion of hydronium ions which may contribute to a reduction in the extraction yield.

Temperature

A study by Feng et al. (2020) found that temperature plays an important role in the extraction of alumina, as an increase in temperature also increased the extraction yield [30]. Higher temperatures provide more thermal energy, promoting particle reactions and increasing kinetic energy. This, in turn, makes it easier to surpass the activation energy barrier required for the reaction to occur [31]. Based on the data presented in Figures 1a(i&ii) and 2a(iii), the effect of temperature on yield exhibited an initial increase followed by a subsequent decrease after reaching 71 °C. The decrease in the yield may be attributed to possible solvent losses during the leaching process, resulting in a lower amount of aluminium sulphate being leached. Notably, a lower leaching temperature resulted in a decreased recovery of aluminium. This is because aluminium tends to be more sensitive to higher temperatures, allowing diffusion processes to continue.

This work's findings contrasted with those of other studies, which mostly showed an increase in yields at higher temperatures ranging from 90 to 100 °C. Sarker et al. (2015) demonstrated that adjusting the temperature within the range of 25 °C to 100 °C, alongside an acid concentration of 4 mol/L, resulted in a notable increase in alumina extraction, specifically from 51 % to 71 % [28]. Similarly, Shi et al. (2023) achieved a comparable result in their study by elevating the temperature from 50 °C to 90 °C, while keeping the acid concentration at 30 wt.% [17].
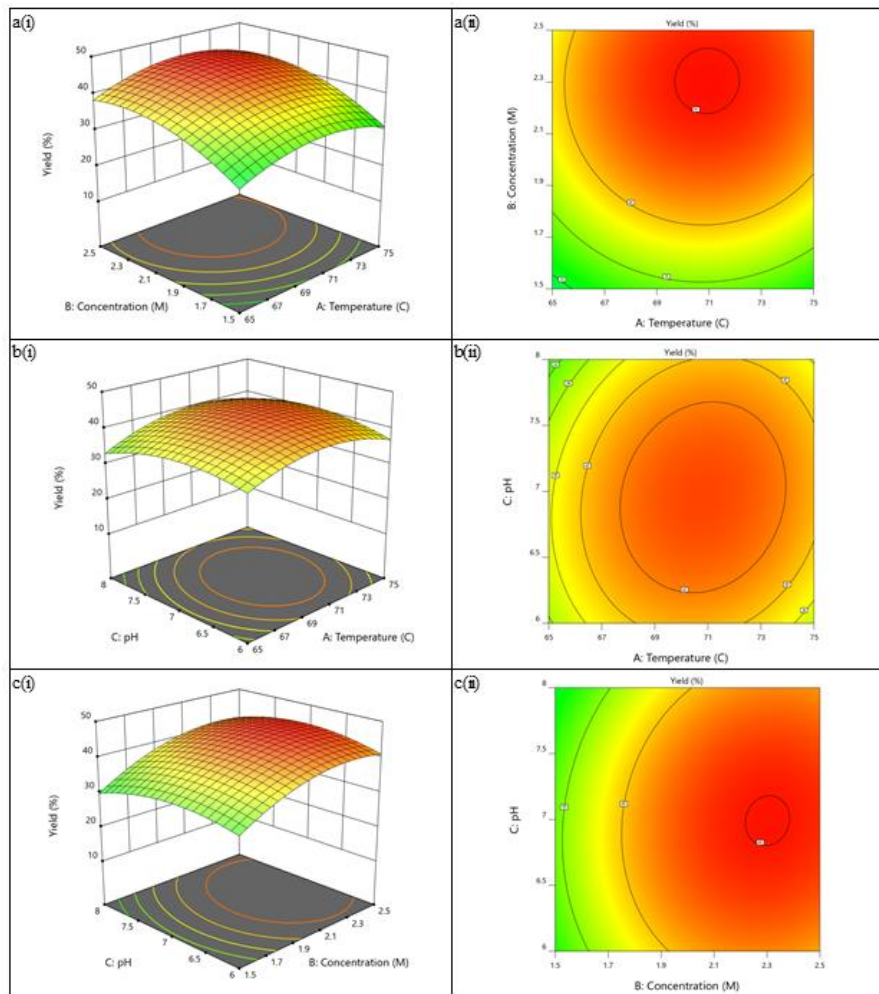
Figure 1. 3D response surface and contour plots for response yields with different a(i & ii) concentrations and temperatures, b(i & ii) pH and temperatures, and c(i & ii) pH and concentrations.

128   Mohamad Jamil Arif Mansor, Yeoh Yuan Xin,
       Siti Nor Amira Rosli, Noor Intan Shafinas Muhammad,
       Shanmuga Kittappa and Sumaiya Zainal Abidin

Process Optimization of Alumina Extraction
from Aluminium Dross Via Response
Surface Methodology
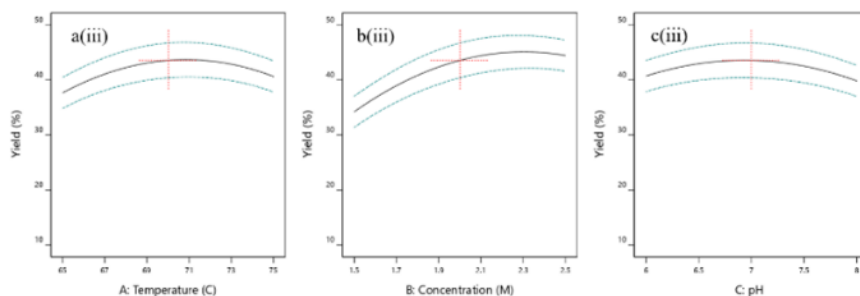
Figure 2. Single responses of every parameter for yield; a(iii) temperature, b(iii) concentration, c(iii) pH.

This modification resulted in a significant improvement in the leaching rate, which increased by a considerable 19 %. A possible explanation for this occurrence may be due to the fact that higher temperatures accelerate the rate of dissolution, leading to a higher concentration of SO^{4-} ions, especially as water vaporizes from the solution [32]. The higher concentration of sulfuric acid leads to a low yield due to an increase in sulphate ions (SO_4^{2-}), as shown in Figure 2b(iii). According to Zhang et al. (2019), the presence of high levels of SO_4^{2-} ions on the oxide surface can result in the formation of a layer of sulphate, which has the potential to impede chemical reactions from taking place.

In summary, the product yield was substantially influenced by both the acid concentration and temperature parameters, as the reaction rate increased at higher temperatures and acid concentrations. However, achieving a higher yield did not necessarily equate to achieving high purity, as the process may be affected by other variables. Therefore, it is essential to monitor and optimize other aspects of the experiment to ensure that the highest possible level of purity is obtained. Furthermore, while the highest yield obtained from the RSM was 45.62 % for single-stage leaching, the implementation of multistage leaching may enhance extraction efficiency and directly improve alumina yield. According to a recent study by Yan et al. (2020), aluminium extraction increased from 88 % to 100 % with the implementation of a four-stage leaching process [33]. A similar trend can be seen in the study by Wang et al. (2018), in which the recovery rate increased to 86.43 % with two-stage leaching. This clearly shows that multistage leaching further improves extraction yields [34].

2.3.   Effect of Parameters on Purity

The ANOVA results (Table 5) demonstrated the statistical significance of the RSM models for purity, as indicated by the p-value. In the present study, the p-value for the model was 0.0003, which is less than 0.05, indicating that the model was highly significant. As indicated in Table 5, there were five significant model terms that impacted the extraction of alumina from aluminium dross. These significant model terms were temperature (A), pH (C), temperature-acid concentration (AB), quadratic term of concentration (B^2), and quadratic term of pH (C^2). Nevertheless, the model term with the utmost significance was pH, which greatly influenced the purity of alumina extracted from aluminium dross, as indicated by the substantial F-value of 62.34. Temperature also played a role in determining purity, as indicated by its F-value of 22.33. However, the contribution of acid concentration to purity was relatively modest, given its lower F-value. The lack of fit F-value of 13.35 suggests that the lack of fit was not significant compared to the pure error. This suggests that the model fit the data well and proficiently captured the interactions among the variables being examined. Moreover, the probability that a lack of fit F-value of this magnitude would occur due to random variation was only 7.11 %. An insignificant lack of fit is a favourable result, signifying that the model effectively elucidated the data. It indicates that the model fit the data well, and would give more accurate conclusions and predictions.

The coded Equation (10) was used to estimate the response based on the significant p-value of a given factor level. In this equation, the high level parameters were assigned as +1, while the low level ones were assigned as −1. The equation determined the significance of each factor by comparing the factor coefficients.

The assumption was made that the null hypothesis (parameters affecting the purity values) was true. Therefore, the p value represented the probability of acquiring outcomes as unusual as the observed outcomes of a statistical hypothesis test. Since the p value was lower than 0.05, it suggests that the parameter or model had a significant effect on the process. Thus, for the same reason as before, a type 1 hypothesis was adopted for this study, recognizing the 5 % or less chance that the result would occur under the null hypothesis. The quadratic model equation for alumina production as a function of alumina purity (%), with variables A for temperature, C for pH, AB for temperature- acid concentration, B^2 for the quadratic term of concentration, and C^2 as the quadratic term for pH, is shown in Equation (10).

$$Purity = 91.47 + 0.875A - 1.4619C - 0.8AB - 0.5142B^2 - 1.5023C^2 \tag{10}$$

129 Mohamad Jamil Arif Mansor, Yeoh Yuan Xin,
Siti Nor Amira Rosli, Noor Intan Shafinas Muhammad,
Shanmuga Kittappa and Sumaiya Zainal Abidin

Process Optimization of Alumina Extraction
from Aluminium Dross Via Response
Surface Methodology

Table 5. ANOVA for purity obtained from (CCD) RSM.

Source	Sum of Squares	df	Mean Square	F-value	p-value	Coefficient Estimate
Model	99.15	9	11.0200	20.09	0.0003	91.4700
A-Temperature	12.25	1	12.2500	22.33	0.0021	0.8750
B-Concentration	0.25	1	0.2450	0.45	0.5253	0.1237
C-pH	34.19	1	34.1900	62.34	< 0.0001	-1.4600
AB	5.12	1	5.1200	9.33	0.0184	-0.8000
AC	0.02	1	0.0200	0.04	0.8540	0.0500
BC	0.32	1	0.3200	0.58	0.4699	0.2000
A²	0.90	1	0.8987	1.64	0.2413	-0.2154
B²	5.12	1	5.1200	9.34	0.0184	-0.5142
C²	43.71	1	43.7100	79.70	< 0.0001	-1.5000
Residual	3.84	7	0.5485			
Lack of Fit	3.73	5	0.7455	13.35	0.0711	
Pure Error	0.11	2	0.0558			

2.4. Response Surface Methodology Graph for Purity

Figure 3 depicts the 3D plots of the response surface methodology (RSM) analysis for three independent parameters influencing the purity of the extracted aluminium. Each response surface plot includes two parameters, while the third parameter was held constant at its mean level. The product's purity was evaluated using XRF analysis.

Temperature and Acid Concentration

Figure 3a(i&ii) illustrates the impact of varying temperatures and acid concentrations on the purity of alumina. Based on the data presented in Figure 3a(i&ii), the highest level of purity in alumina was achieved at a temperature of 70 °C and an acid concentration of 2 M. However, as the acid concentration and temperature were increased further, the purity of Al_2O_3 decreased. According to a study by Yang et al. (2019), temperature changes had a notable impact on the rate of aluminium dissolution, as opposed to aluminium leaching [35]. The investigation involved altering the temperature from 25 °C (298.15 K) to 100 °C (373.15 K) while maintaining an acid concentration of 3.91 mol/L. The results indicated a rise in the aluminium leaching rate up to 80 °C, followed by a subsequent decline beyond this threshold. This trend may be linked to the contrasting effects of thermodynamics and kinetics, as suggested in the existing literature [36]. Essentially, raising the leaching temperature affects the rate of reaction and increases the extent to which the leaching process occurs, resulting in a more comprehensive dissolution [36,37].

The results also show that temperature increases at lower acid concentrations resulted in higher purity levels. This is because during the dissolution process, specific metal ions such as aluminium, are primarily extracted at lower acid concentrations. As the acid concentration rises, less metal can be recovered due to the entrapment of certain soluble metal sulphates in the residue [38]. Furthermore, the leachate contains a higher concentration of additional metals, primarily due to the increased acid concentration. It was evident in the XRF analysis that the solubility of metallic iron was enhanced in acidic conditions, based on the elemental composition of the final product [38].

pH Precipitation

Figure 3b(i&ii) illustrates the impact of pH precipitation and temperature, while Figure 3c(i&ii) demonstrates the correlation between pH and acid concentration on the purity. Both figures collectively support the conclusion that pH significantly influenced the purity of alumina. The combined observations from Figure 3b(i&ii) and c(i&ii) suggest that the purity of alumina improved when subjected to lower pH conditions. Conversely, findings obtained at higher pH levels showed an increased release of elements into the final product. Raising the pH value elevated the solution's ammonia concentration, leading to the generation of more side reactions. In accordance with the reactivity series, aluminium demonstrates higher reactivity relative to iron. This dissimilarity is the cause behind the prioritized reaction of aluminium ions, resulting in the formation of aluminium hydroxide ($Al(OH)_3$) as illustrated in Equation (11). A similar outcome was obtained by another study, where an increase in pH from 7 to 12 led to a decline in aluminium content, accompanied by elevated levels of sodium, sulphur, and other elements [32].

pH exerted a notable influence on the colour of the alumina precursor. This phenomenon can be explained by Equations (12) and (13), where under lower pH conditions, the ferrous (Fe^{2+}) and ferric (Fe^{3+}) ions start to precipitate. According to Wei

130   Mohamad Jamil Arif Mansor, Yeoh Yuan Xin,
       Siti Nor Amira Rosli, Noor Intan Shafinas Muhammad,
       Shanmuga Kittappa and Sumaiya Zainal Abidin

Process Optimization of Alumina Extraction
from Aluminium Dross Via Response
Surface Methodology

et al. (2005), Fe^{2+} and Fe^{3+} ions oxidize at pH 3.5 – 4 [39]. Moreover, at a higher pH, Fe^{2+} and Fe^{3+} will react with excess ammonia to produce more iron hydroxide (orange colour) that contributes to lower purity values. This observation is similar to the study by Zhang et al. (2019) where more alkaline conditions (pH 9 – 12) affected and reduced aluminium content due to other elements in the sample [32]. The presence of iron plays a crucial role in achieving higher purity alumina in alkaline conditions. Thus, a higher pH value had a significant effect on purity [39].

$$Al^{3+}(aq) + 3NH_3(aq) + 3H_2O(aq) \rightleftharpoons Al(OH)_3(s) + 3NH^{+4}(aq) \tag{11}$$

$$Fe^{2+}(aq) + 2NH_3(aq) + 3H_2O(l) \rightleftharpoons Fe(OH)_2(s) + 2NH^{+4}(aq) \tag{12}$$

$$Fe^{3+}(aq) + 3NH_3(aq) + 3H_2O(l) \rightleftharpoons Fe(OH)_2(s) + 3NH^{+4}(aq) \tag{13}$$
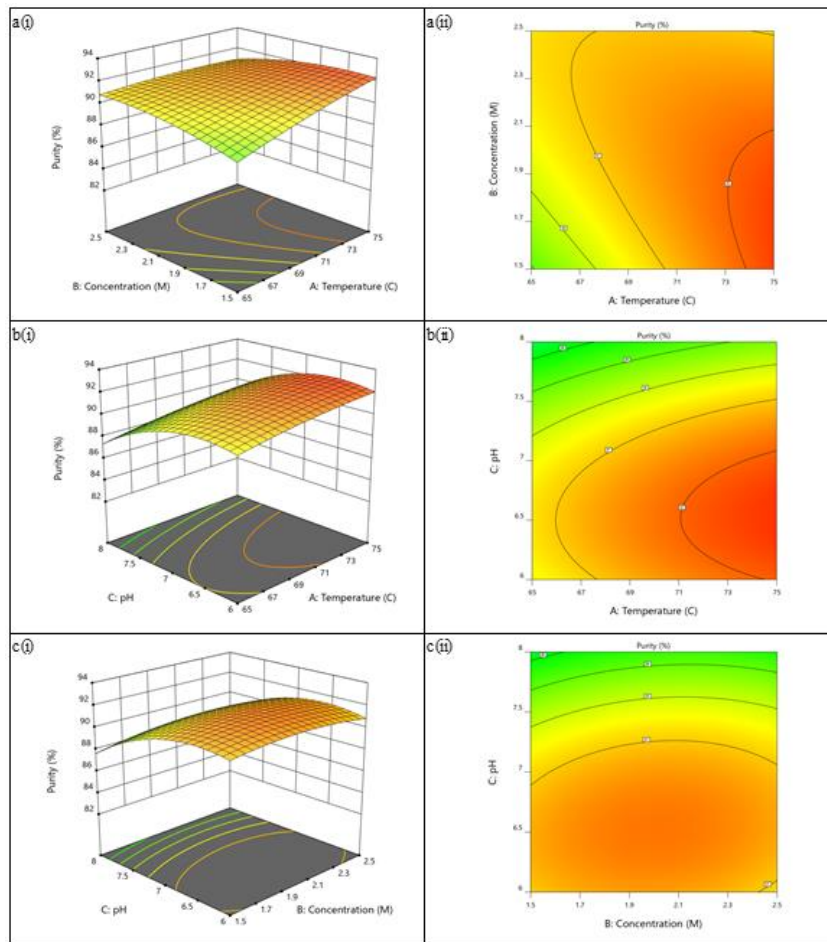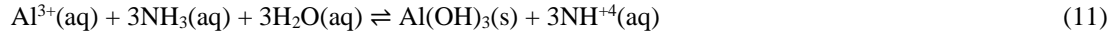
Figure 3. 3D response surface and contour plots for purity at different a(i & ii) concentrations and temperatures, b(i & ii) pH and temperatures, and c(i & ii) pH and concentrations.
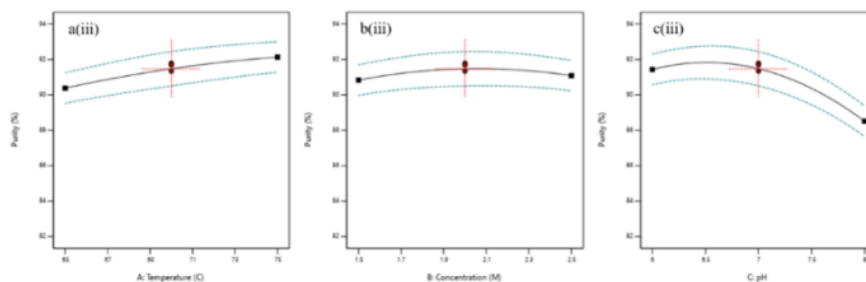
Figure 4. Single response of every parameter for purity; a(iii) temperature, b(iii) concentration, c(iii) pH.

131   Mohamad Jamil Arif Mansor, Yeoh Yuan Xin,
Siti Nor Amira Rosli, Noor Intan Shafinas Muhammad,
Shanmuga Kittappa and Sumaiya Zainal Abidin

Process Optimization of Alumina Extraction
from Aluminium Dross Via Response
Surface Methodology

Acid Concentration

By analyzing the data presented in Figures 3a(i&ii), 3c(i&ii), and 4b(iii), it is evident that the purity of aluminium hydroxide ($Al(OH)_3$) was directly impacted by the acid concentration. As shown in Figure 4b(iii), the purity gradually increased with acid concentrations of 1.5 to 2 M and started decreasing from 2 M to 2.5 M. The results of Benkhelif et al. (2022) demonstrated a similar pattern, in which the alumina recovery percentage exhibited an increase with acid concentration (3 % – 15 %), ultimately achieving a purity level of 99.2 % when the H_2SO_4 concentration surpassed 15 %, and then the purity decreased to 77.1 % at 40 % [36]. The rise in alumina content is attributed to the solubility of aluminium compounds in the acidic solution. On the other hand, the reduction in purity can be attributed to two underlying factors. According to Benkhelif et al. (2022), this decrement may stem from an insufficient supply of Al^{3+} cations, hindering their reaction with SO_4^{2-} and subsequent conversion into alumina [36]. From a different perspective, as proposed by Sarker et al. (2015), it is conceivable that the presence of Al^{3+} ions could impede H^+ diffusion at higher concentrations, leading to a decline in purity [28].

2.5. Optimum Conditions and Validation

DE software was used to design and simulate all the parameters to optimize the experimental conditions. The ideal conditions recommended by the DE software for producing alumina were: a leaching temperature of 71.53 °C, an acid concentration of 2.19 M, and a pH of 6.43 for precipitation. After obtaining the recommended experimental parameters, the subsequent phase entailed conducting experiments to evaluate their

effectiveness. This step was crucial for confirming the precision and dependability of the DE suggestions, ensuring their practical applicability in the experimental context. Table 6 displays a notable difference in both the purity and yield obtained from the experimental results when compared to the predicted values generated by the software. The achieved experimental yield was 42.17 %, slightly below the anticipated software-predicted value of 44.72 %, a deviation of 2.55 %. Similarly, the attained experimental purity stood at 91.90 %, exceeding the software-generated predicted purity of 91.86 %, a deviation of -0.04%. These results indicates that the predicted values provided by RSM were very similar to the experimental values.

3. Aluminium Oxide Characterization

The alumina extracted under the optimal conditions was subsequently subjected to characterization techniques such as XRF, XRD, and BET analysis. XRF analysis was used to analyze the composition of the product, XRD analysis was used to determine the phases present in the sample, while BET analysis was used to determine the porosity and the surface area of the sample.

3.1. XRF Analysis

Table 7 shows the chemical composition of extracted alumina in wt.%. The outcome revealed that the extracted material was composed primarily of Al_2O_3 (91.90 %). This finding signifies the effectiveness of the extraction process in successfully isolating and purifying the targeted alumina compound. Other oxides present in minor quantities were CaO (0.162 %), FeO (3.696 %), K_2O (0.129 %), SiO (0.701 %), SO_2 (1.223 %), TiO_2 (0.188 %) and others (2.001 %).

Table 6. Experimental validation for optimum conditions suggested by CCD.

Type of data	Factor 1 A: Temperature °C	Factor 2 B: Concentration M	Factor 3 C: pH of precipitation	Response 1: Yield %	Response 2: Purity %
Predicted	71.53	2.19	6.43	44.72	91.86
Experimental	71.50	2.20	6.50	42.17	91.90
Error %				**2.55**	**0.04**

Table 7. Chemical composition of extracted alumina in wt%.

Oxides							
Al_2O_3	CaO	Fe_2O_3	K_2O	SO_2	SiO	TiO_2	Others
91.900	0.162	3.696	0.129	1.223	0.701	0.1880	2.001

132   Mohamad Jamil Arif Mansor, Yeoh Yuan Xin,
        Siti Nor Amira Rosli, Noor Intan Shafinas Muhammad,
        Shanmuga Kittappa and Sumaiya Zainal Abidin

Process Optimization of Alumina Extraction
from Aluminium Dross Via Response
Surface Methodology

3.2.   XRD Analysis

In Figure 5, the X-ray diffractogram of the alumina sample reveals the structural complexity of Al_2O_3, an intriguing oxide with a composition that encompasses multiple metastable phases. These phases consist of gamma-(γ), theta-(θ), kappa-(κ), and alpha-(α) Al_2O_3. At 700 °C, XRD analysis revealed the presence of several phases of alumina in the extracted sample. The identified phases include γ-Al_2O_3 observed at 2θ = 34.14°, 37.51° and 45.86°, as well as α-Al_2O_3 observed at 2θ = 25.33°, 33.72° and 36.28°. These γ and α phases were similar to those reported by Roslan et al. (2019) [23] and How et al. (2017) [22]. θ-Al_2O_3 was observed at 2θ = 21.21°, 31.17°, 45.74°, 46.48°, 60.19° and 62.11° (JCPSD No: 00-056-0456), and κ-Al_2O_3 at 2θ =29.64°, 40.86°, 48.68°, and 55.38° (JCPSD No: 00-052-0803). The predominant phase present in this sample was θ, followed by α, κ, and γ. However, there were some traces in the sample of iron oxide, which was observed at 2θ = 53.52°, 56.99°, and 74.10° [40].

Several studies have stated that the phase composition of alumina is influenced by the temperature of calcination [41]. Roslan et al. (2019) provided insights into the presence of different phases at varying temperatures [23]. In this study, XRD analysis demonstrated that at lower calcination temperatures (700 °C), the predominant phase observed was gamma (γ). However, as the calcination temperature increased within the range of 800 – 1,000 °C, additional phases such as theta (θ), kappa (κ), and alpha (α) appeared [23]. Contrary to this, research by Mishra (2002) indicated that the pure alpha phase of alumina could be achieved at temperatures lower than 1,000 °C [42]. However, it is crucial to minimize the presence of impurities to obtain pure alpha alumina without other phases such as theta (θ), kappa (κ) and gamma (γ) [42]. Based on the results obtained, it can be observed that the most common phase was the alpha phase ($\theta > \alpha > \kappa > \gamma$). This may be due to the presence of impurities in alumina, as Roslan et al. (2019) stated that sequencing of the phase also depends on the granulometry of the alumina precursor [23]. The presence of impurities in aluminium oxide has the potential to alter the temperature needed for phase transitions, leading to an increase or decrease in the threshold, while also exerting an influence on the kinetics of the alumina phase.

3.3.   BET Surface Area

The BET surface area for Al_2O_3 obtained under the optimum extraction conditions was 123.12 m^2/g, as shown in Table 8. This closely aligns with the results of How et al. (2017), who reported a range of BET surface area values between 111.1 and 128.1 m^2/g [22]. The Al_2O_3 surface area is highly dependent on the dissolution of Al_2O_3 during the aging process that is affected by pH precipitation and the extent of aggregation [43]. In the current study, the BET surface area range varied depending on the precipitation pH, specifically within the range of pH 5 to 9. During the validation experiments, a pH of 7 was used, resulting in the aforementioned BET surface area of 123.12 m^2/g. This shows that Al_2O_3 extracted from aluminium dross is as a highly versatile and valuable material with significant applications in the sector of catalysis and adsorption. This unique form of alumina exhibits exceptional properties, including a remarkably high surface area and finely tuned particle size, which make it a sought-after choice for diverse industrial applications.
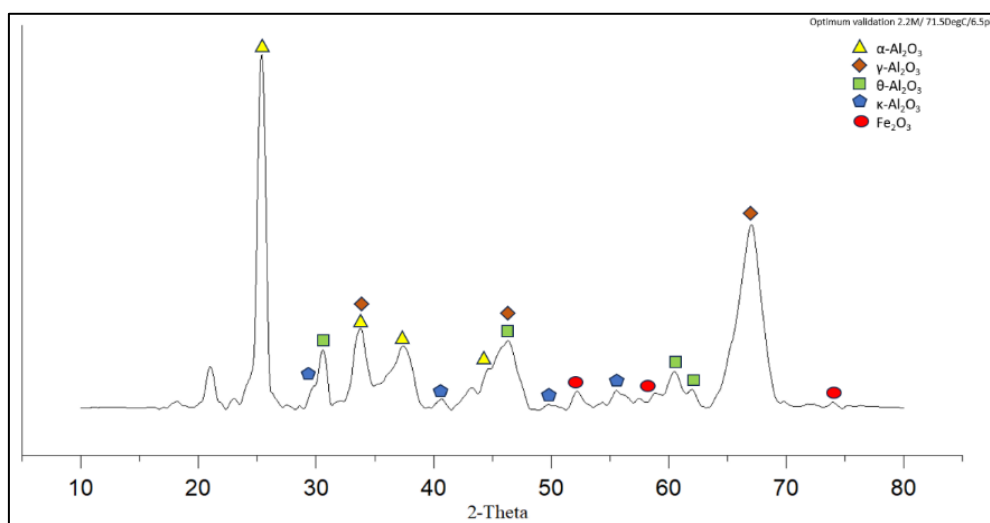
Figure 5. X-ray diffractogram of Al_2O_3 extracted under optimum conditions (71.5 °C, 2.2 M, and pH 6.5).

133   Mohamad Jamil Arif Mansor, Yeoh Yuan Xin,
Siti Nor Amira Rosli, Noor Intan Shafinas Muhammad,
Shanmuga Kittappa and Sumaiya Zainal Abidin

Process Optimization of Alumina Extraction
from Aluminium Dross Via Response
Surface Methodology

CONCLUSION

This work exemplifies the successful utilization of the CCD optimization technique within the RSM framework. Through the implementation of a quadratic model, this study effectively modelled the extraction of alumina from AD. Through the application of Design Expert software, an exploration was conducted into the impacts of different parameters on the production of alumina from AD. This unique optimization method has not been extensively reported in previous studies. According to the analysis performed using the software, the most favourable conditions for extracting alumina from aluminium dross were an acid concentration of 2.2 M, 71.5 °C leaching temperature, and precipitation pH of 6.5. The resulting optimum yield and purity of alumina extracted from AD were found to be 42.17 % and 91.90 %, respectively. The results of this study provide valuable insights that contribute to the improvement of alumina production from aluminium dross, especially the successful determination of the most favourable extraction conditions while determining which factors had significant influence on alumina quality as well as quantity. The research also indicated that to enhance the extraction yield, it is advisable to implement a multistage leaching process. Multistage leaching involves repetition of the extraction process with multiple steps or stages, which enhances alumina recovery. Overall, these findings create an opportunity for industrial waste management to recycle aluminium dross efficiently and cost-effectively, and is an attractive option to reduce waste.

ACKNOWLEDGEMENTS

REFERENCES

1. Brough, D. and Jouhara, H. (2020) The aluminium industry: A review on state-of-the-art technologies, environmental impacts and possibilities for waste heat recovery. *International Journal of Thermo-fluids*, **1–2**, 100007. https://doi.org/10.1016/j.ijft.2019.100007.

2. Wang, M., Liu, G., Jiang, X., Li, S., Liu, W. and Zheng, M. (2016) Formation and emission of brominated dioxins and furans during secondary aluminum smelting processes. *Chemosphere*, **146**, 60–67. 10.1016/J.CHEMOSPHERE.2015.11.109.

3. Dash, B., Das, B., Tripathy, B., Bhattacharya, I. and Das, S. (2008) Acid dissolution of alumina from waste aluminium dross. *Hydrometallurgy*, **92**, 48–53.

4. Amer, A. M. (2002) Extracting aluminum from dross tailings. *JOM*, **54**, 72–75. 10.1007/BF02709754.

5. Shen, H., Liu, B., Ekberg, C. and Zhang, S. (2021) Harmless disposal and resource utilization for secondary aluminum dross: A review. *Science of The Total Environment*, **760**, 143968. https://doi.org/10.1016/j.scitotenv.2020.143968.

6. Verma, S. K., Dwivedi, V. K. and Dwivedi, S. P. (2020) Utilization of aluminium dross for the development of valuable product - A review. *In Materials Today: Proceedings (Elsevier Ltd)*, 547–550. 10.1016/j.matpr.2020.12.045.

7. Lin, W. C., Tsai, C. H., Zhang, D. N., Syu, S. S. and Kuo, Y. M. (2022) Recycling of aluminum dross for producing calcinated alumina by microwave plasma. *Sustainable Environment Research*, **32**. 10.1186/s42834-022-00160-9.

8. Huang, K., Wang, L., Li, M., Mi, T., Zhang, J., Liu, J. and Yi, X. (2023) Mechanism of porous ceramic fabrication using Second Aluminum Dross assisted by corn stalk as pore-forming agent. *Environ. Technol. Innov.*, **31**. 10.1016/J.ETI. 2023.103195.

9. Tsakiridis, P. E. (2012) Aluminium salt slag characterization and utilization – A review. *J. Hazard Mater.*, **217–218**, 1–10. 10.1016/J.JHAZMAT. 2012.03.052.

10. Mahinroosta, M. and Allahverdi, A. (2018) Hazardous aluminum dross characterization and recycling strategies: A critical review. *J. Environ. Manage*, **223**, 452–468. https://doi.org/10.1016/j.jenvman.2018.06.068.

11. Huang, K. and Yi, X. (2023) Resource Utilization and High-Value Targeted Conversion for Secondary Aluminum Dross: A Review. *JOM*, **75**, 279–290. 10.1007/s11837-022-05560-1.

12. Tunca, B., Alüminyum, Z. and Tic, S. A. Ş. (2020) Synthesize of the γ-Al 2 O 3 (Alumina) from Aluminium Dross by Using Chemical Method Merve Özcan. *International Refereed Journal of Engineering and Science*, **9**, 25–32.

13. Zhu, X., Yang, J., Yang, Y., Huang, Q. and Liu, T. (2022) Pyrometallurgical process and multi-pollutant co-conversion for secondary aluminum dross: a review. *Journal of Materials Research*

134   Mohamad Jamil Arif Mansor, Yeoh Yuan Xin,
Siti Nor Amira Rosli, Noor Intan Shafinas Muhammad,
Shanmuga Kittappa and Sumaiya Zainal Abidin

Process Optimization of Alumina Extraction
from Aluminium Dross Via Response
Surface Methodology

and Technology, **21**, 1196–1211. 10.1016/J.JMRT. 2022. 09.089.

14. Lv, H., Xie, M., Wu, Z., Li, L., Yang, R., Han, J., Liu, F. and Zhao, H. (2022) Effective Extraction of the Al Element from Secondary Aluminum Dross Using a Combined Dry Pressing and Alkaline Roasting Process. *Materials*, **15**, 10.3390/ma15165686.

15. Meshram, A. and Singh, K. K. (2018) Recovery of valuable products from hazardous aluminum dross: A review. *Resour. Conserv. Recycl.*, **130**, 95–108.

16. Mahinroosta, M. and Allahverdi, A. (2018) Enhanced alumina recovery from secondary aluminum dross for high purity nanostructured γ-alumina powder production: Kinetic study. *J. Environ. Manage*, **212**, 278–291. 10.1016/j.jenvman.2018.02.009.

17. Shi, M., Yu, A. and Li, Y. (2023) Production of Alumina from Secondary Aluminum Dross by Hydrometallurgical Process. *JOM*, **75**, 291–300. 10.1007/s11837-022-05599-0.

18. Qiu, T., Yan, H., Li, J., Liu, Q. and Ai, G. (2018) Response surface method for optimization of leaching of a low-grade ionic rare earth ore. *Powder Technol.*, **330**, 330–338. https://doi.org/10.1016/j.powtec.2018.02.044.

19. Wei, X., Gao, Y., Han, J., Wang, Y. and Qin, W. (2023) Optimisation of extraction of valuable metals from waste LED via response surface method. *Transactions of Nonferrous Metals Society of China*, **33**, 938–950. https://doi.org/10.1016/S1003-6326(23)66157-6.

20. Rautela, R., Yadav, B. R. and Kumar, S. (2024) Enhancing the efficiency of metals extraction from waste lithium-ion batteries through glycine leaching using response surface methodology for economic feasibility. *J. Clean. Prod.*, **447**, 141602. https://doi.org/10.1016/j.jclepro.2024.141602.

21. Kolbadinejad, S. and Ghaemi, A. (2024) Optimization of atmospheric leaching parameters for cadmium and zinc recovery from low-grade waste by response surface methodology (RSM*). Sci. Rep.*, **14**. 10.1038/s41598-024-52088-2.

22. How, L. F., Islam, A., Jaafar, M. S. and Taufiq-Yap, Y. H. (2017) Extraction and Characterization of Γ-Alumina from Waste Aluminium Dross. *Waste Biomass Valorization*, **8**, 321–327. 10.1007/s12649-016-9591-4.

23. Roslan, N. A., Abidin, S. Z., Nasir, N. S., Chin, S. Y. and Taufiq-Yap, Y. H. (2019) Extracted ?-

Al2O3from aluminum dross as a catalyst support for glycerol dry reforming reaction. In Materials Today: *Proceedings (Elsevier Ltd)*, 63–68. 10.1016/j.matpr.2020.09.390.

24. Mohamad, S. M., Roslan, N. A. and Zainal Abidin, S. (2022) Comparison on the physicochemical properties of alumina extracted from various aluminum wastes. *Mater. Today Proc.*, **57**, 1179–1183. https://doi.org/10.1016/j.matpr.2021.09.561.

25. Das, B. R., Dash, B., Tripathy, B. C., Bhattacharya, I. N. and Das, S. C. (2007) Production of η-alumina from waste aluminium dross. *Miner. Eng.*, **20**, 252–258. https://doi.org/10.1016/j.mineng.2006.09.002.

26. Chaker, H., Ameur, N., Saidi-Bendahou, K., Djennas, M. and Fourmentin, S. (2021) Modeling and Box-Behnken design optimization of photo-catalytic parameters for efficient removal of dye by lanthanum-doped mesoporous TiO2. *J. Environ. Chem. Eng.*, **9**, 104584. https://doi.org/10.1016/j.jece.2020.104584.

27. Matinde, E., Simate, G. S. and Ndlovu, S. (2018) Mining and metallurgical wastes: a review of recycling and re-use practices.

28. Sarker, M. S. R., Alam, M. Z., Qadir, M. R., Gafur, M. A. and Moniruzzaman, M. (2015) Extraction and characterization of alumina nanopowders from aluminum dross by acid dissolution process. *International Journal of Minerals, Metallurgy and Materials*, **22**, 429–436. 10.1007/s12613-015-1090-2.

29. Al-Zahrani, A. A. and Abdul-Majid, M. H. (2009) Extraction of Alumina from Local Clays by Hydrochloric Acid Process. *JKAU: Eng. Sci.*, **20**, 29–41.

30. Feng, H., Zhang, G., Yang, Q., Xun, L., Zhen, S. and Liu, D. (2020) The investigation of optimizing leaching efficiency of al in secondary aluminum dross via pretreatment operations. *Processes*, **8**, 1–13. 10.3390/PR8101269.

31. Kohitlhetse, I., Thubakgale, K., Mendonidis, P. and Manono, M. (2021) Investigating the Effect of Reaction Temperature on the Extraction of Calcium from Ironmaking Slag: A Kinetics Study. *Environmental Sciences Proceedings 2021*, **6**, 31. 10.3390/IECMS2021-09366.

32. Zhang, S., Zhu, W., Li, Q., Zhang, W. and Yi, X. (2019) Recycling of Secondary Aluminum Dross to Fabricate Porous Assisted by Corn Straw as Biotemplate. *Journal of Materials Science and Chemical Engineering*, **07**, 87–102. 10.4236/msce.2019.712010.

135   Mohamad Jamil Arif Mansor, Yeoh Yuan Xin,
Siti Nor Amira Rosli, Noor Intan Shafinas Muhammad,
Shanmuga Kittappa and Sumaiya Zainal Abidin

Process Optimization of Alumina Extraction
from Aluminium Dross Via Response
Surface Methodology

33. Yan, Y., Wang, K., Clough, P. T. and Anthony, E. J. (2020) Developments in calcium/chemical looping and metal oxide redox cycles for high-temperature thermochemical energy storage: A review. *Fuel Processing Technology*, **199**. 10.1016/j.fuproc.2019.106280.

34. Wang, Y., Wang, Y., Su, X., Zhou, H., and Sun, X. (2018) Complete separation of aluminium from rare earths using two-stage solvent extraction. *Hydrometallurgy*, **179**, 181–187. 10.1016/j. hydromet.2018.06.004.

35. Yang, Q., Li, Q., Zhang, G., Shi, Q. and Feng, H. (2019) Investigation of leaching kinetics of aluminum extraction from secondary aluminum dross with use of hydrochloric acid. *Hydro-metallurgy*, **187**, 158–167. 10.1016/J.HYDRO MET. 2019.05.017.

36. Benkhelif, A., Kolli, M. and Hamidouche, M. (2022) Synthesis of Submicronic α-Alumina from Local Aluminum Slags. *Journal of Mining and Metallurgy, Section B: Metallurgy*, **58**, 17–127. 10.2298/JMMB210401053B.

37. Zong, Y., Li, F., Chen, W. and Liu, Z. (2019) Extraction of alumina from high alumina coal ash using an alkaline hydrothermal method. *SN Appl. Sci.*, **1**. 10.1007/s42452-019-0814-8.

38. Huang, F., Liao, Y., Zhou, J., Wang, Y. and Li, H. (2015) Selective recovery of valuable metals from nickel converter slag at elevated temperature with sulfuric acid solution. *Sep. Purif. Technol.*, **156**, 572–581. 10.1016/j.seppur.2015.10.051.

39. Wei, X., Viadero, R. C. and Buzby, K. M. (2005) Recovery of iron and aluminum from acid mine drainage by selective precipitation. *Environ. Eng. Sci.*, **22**, 745–755. 10.1089/ees.2005.22.745.

40. Mishra, A. and Sardar, M. (2014) Isolation of Genomic DNA by Silane-Modified Iron Oxide Nanoparticles.

41. Rogojan, R., Andronescu, E., Ghiţulică, C., Vasile, B. Ş. and Vasile, B. Ş. (2011) Synthesis and Characterization of Alumina Nano-Powder Obtained by Sol-Gel Method. *Bull. Series B., **73**.*

42. Mishra, P. (2002) Low-temperature synthesis of α-alumina from aluminum salt and urea. *Mater. Lett.*, **55**, 425–429. https://doi.org/10.1016/ S0167-577X(02)00491-3.

43. Hellgardt, K. and Chadwick, D. (1998) Effect of pH of Precipitation on the Preparation of High Surface Area Aluminas from Nitrate Solutions. *Ind. Eng. Chem. Res.*, **37**, 405–411. 10.1021/ IE970591A.